

# Identifying the Best Machine Learning Algorithms for Brain Tumor Segmentation, Progression Assessment, and Overall Survival Prediction in the BRATS Challenge

Spyridon Bakas<sup>1,2,†,‡,\*</sup>, Mauricio Reyes<sup>3,†</sup>, Andras Jakab<sup>4,†,‡</sup>, Stefan Bauer<sup>3,5,†</sup>, Markus Rempfler<sup>8,64,126,†</sup>, Alessandro Crimi<sup>6,†</sup>, Russell Takeshi Shinohara<sup>1,7,†</sup>, Christoph Berger<sup>8,†</sup>, Sung Min Ha<sup>1,2,†</sup>, Martin Rozycki<sup>1,2,†</sup>, Marcel Prastawa<sup>9,†</sup>, Esther Alberts<sup>8,64,126,†</sup>, Jana Lipkova<sup>8,64,126,†</sup>, John Freymann<sup>10,11,‡</sup>, Justin Kirby<sup>10,11,‡</sup>, Michel Bilello<sup>1,2,‡</sup>, Hassan Fathallah-Shaykh<sup>12,‡</sup>, Roland Wiest<sup>3,5,‡</sup>, Jan Kirschke<sup>125,‡</sup>, Benedikt Wiestler<sup>125,‡</sup>, Rivka Colen<sup>13,‡</sup>, Aikaterini Kotrotsou<sup>13,‡</sup>, Pamela Lamontagne<sup>14,‡</sup>, Daniel Marcus<sup>15,16,‡</sup>, Mikhail Milchenko<sup>15,16,‡</sup>, Arash Nazeri<sup>16,‡</sup>, Marc-Andre Weber<sup>17,‡</sup>, Abhishek Mahajan<sup>18,‡</sup>, Ujjwal Baid<sup>19,‡</sup>, Dongjin Kwon<sup>1,2,†</sup>, Manu Agarwal<sup>108</sup>, Mahbubul Alam<sup>32</sup>, Alberto Albiol<sup>33</sup>, Antonio Albiol<sup>33</sup>, Varghese Alex<sup>106</sup>, Tuan Anh Tran<sup>102</sup>, Tal Arbel<sup>91</sup>, Aaron Avery<sup>59</sup>, Pranjal B.<sup>106</sup>, Subhashis Banerjee<sup>35,36</sup>, Thomas Batchelder<sup>32</sup>, Kayhan Batmanghelich<sup>87</sup>, Enzo Battistella<sup>41,42</sup>, Martin Bendszus<sup>22</sup>, Eze Benson<sup>37</sup>, Jose Bernal<sup>39</sup>, George Biros<sup>61</sup>, Mariano Cabezas<sup>39</sup>, Siddhartha Chandra<sup>41</sup>, Yi-Ju Chang<sup>44</sup>, Joseph Chazalon<sup>28</sup>, Shengcong Chen<sup>24</sup>, Wei Chen<sup>45</sup>, Jefferson Chen<sup>79</sup>, Kun Cheng<sup>119</sup>, Meinel Christoph<sup>94</sup>, Roger Chylla<sup>59</sup>, Albert Clérigues<sup>39</sup>, Anthony Costa<sup>121</sup>, Xiaomeng Cui<sup>114</sup>, Zhenzhen Dai<sup>40</sup>, Lutao Dai<sup>49</sup>, Eric Deutsch<sup>42</sup>, Changxing Ding<sup>24</sup>, Chao Dong<sup>64</sup>, Wojciech Dudzik<sup>70,71</sup>, Théo Estienne<sup>41,42</sup>, Hyung Eun Shin<sup>120</sup>, Richard Everson<sup>86</sup>, Jonathan Fabrizio<sup>28</sup>, Longwei Fang<sup>53,54</sup>, Xue Feng<sup>67</sup>, Lucas Fidon<sup>41</sup>, Naomi Fridman<sup>56</sup>, Huan Fu<sup>89</sup>, David Fuentes<sup>57</sup>, David G Gering<sup>59</sup>, Yaozong Gao<sup>67</sup>, Evan Gates<sup>57</sup>, Amir Gholami<sup>60</sup>, Mingming Gong<sup>87,88</sup>, Sandra González-Villá<sup>39</sup>, J. Gregory Pauloski<sup>57</sup>, Yuanfang Guan<sup>107</sup>, Sheng Guo<sup>63</sup>, Sudeep Gupta<sup>18</sup>, Meenakshi H Thakur<sup>18</sup>, Klaus H. Maier-Hein<sup>21</sup>, Woo-Sup Han<sup>62</sup>, Huiguang He<sup>53,54,55</sup>, Aura Hernández-Sabaté<sup>99</sup>, Evelyn Herrmann<sup>101</sup>, Naveen Himthani<sup>61</sup>, Winston Hsu<sup>110</sup>, Cheyu Hsu<sup>110</sup>, Xiaojun Hu<sup>63</sup>, Xiaobin Hu<sup>64</sup>, Yan Hu<sup>65</sup>, Yifan Hu<sup>116</sup>, Rui Hua<sup>67,68</sup>, Teng-Yi Huang<sup>44</sup>, Weilin Huang<sup>63</sup>, Quan Huo<sup>67</sup>, Vivek HV<sup>69</sup>, Fabian Isensee<sup>21</sup>, Mobarakol Islam<sup>80,81</sup>, Francisco J. Albiol<sup>34</sup>, Chiatse J. Wang<sup>110</sup>, Sachin Jambawalikar<sup>47</sup>, V Jeya Maria Jose<sup>81,82</sup>, Weijian Jian<sup>118</sup>, Peter Jin<sup>60</sup>, Alain Jungo<sup>3</sup>, Nicholas K Nuechterlein<sup>90</sup>, Po-Yu Kao<sup>78</sup>, Adel Kermi<sup>73</sup>, Kurt Keutzer<sup>60</sup>, Mahendra Khened<sup>106</sup>, Philipp Kickingeder<sup>22</sup>, Nik King<sup>59</sup>, Haley Knapp<sup>59</sup>, Urspeter Knecht<sup>3</sup>, Lisa Kohli<sup>59</sup>, Deren Kong<sup>63</sup>, Xiangmao Kong<sup>114</sup>, Simon Koppers<sup>31</sup>, Avinash Kori<sup>106</sup>, Ganapathy Krishnamurthi<sup>106</sup>, Piyush Kumar<sup>46</sup>, Kaisar Kushibar<sup>39</sup>, Dmitrii Lachinov<sup>83,84</sup>, Joon Lee<sup>40</sup>, Chengen Lee<sup>110</sup>, Yuehchou Lee<sup>110</sup>, Szidonia Lefkovits<sup>95</sup>, Laszlo Lefkovits<sup>96</sup>, Tengfei Li<sup>50</sup>, Hongwei Li<sup>64</sup>, Wenqi Li<sup>75,76</sup>, Hongyang Li<sup>107</sup>, Xiaochuan Li<sup>109</sup>, Zheng-Shen Lin<sup>44</sup>, Fengming Lin<sup>114</sup>, Chang Liu<sup>40</sup>, Boqiang Liu<sup>45</sup>, Xiang Liu<sup>66</sup>, Mingyuan Liu<sup>113</sup>, Ju Liu<sup>114,115</sup>, Xavier Lladó<sup>39</sup>, Lin Luo<sup>30</sup>, Khan M. Iftekharruddin<sup>32</sup>, Yuhsiang M. Tsai<sup>110</sup>, Jun Ma<sup>72</sup>, Kai Ma<sup>116</sup>, Thomas Mackie<sup>59</sup>, Issam Mahmoudi<sup>73</sup>, Michal Marcinkiewicz<sup>70</sup>, Richard McKinley<sup>5</sup>, Sachin Mehta<sup>90</sup>, Raghav Mehta<sup>91</sup>, Raphael Meier<sup>5</sup>, Dorit Merhof<sup>31</sup>, Craig Meyer<sup>26,27</sup>, Sushmita Mitra<sup>35</sup>, Aliasgar Moiyadi<sup>18</sup>, Grzegorz Mrukwa<sup>70,71</sup>, Miguel A.B. Monteiro<sup>104</sup>, Andriy Myronenko<sup>20</sup>, Eric N Carver<sup>40</sup>, Jakub Nalepa<sup>70,71</sup>, Thuyen Ngo<sup>78</sup>, Chen Niu<sup>66</sup>, Eric Oermann<sup>121</sup>, Arlindo Oliveira<sup>104,105</sup>, Arnau Oliver<sup>39</sup>, Sebastien Ourselin<sup>75</sup>, Andrew P. French<sup>37,38</sup>, Michael P. Pound<sup>37</sup>, Tony P. Pridmore<sup>37</sup>, Juan Pablo Serrano-Rubio<sup>85</sup>, Nikos Paragios<sup>41,43</sup>, Brad Paschke<sup>59</sup>, Linmim Pei<sup>32</sup>, Suting Peng<sup>45</sup>, Bao Pham<sup>103</sup>, Gemma Piella<sup>100</sup>, G.N. Pillai<sup>108</sup>, Marie Piraud<sup>64</sup>, Anmol Popli<sup>108</sup>, Vesna Prčkovska<sup>98</sup>, Santi Puch<sup>98</sup>, Élodie Puybareau<sup>28</sup>, Xu Qiao<sup>45</sup>, Yannick R Suter<sup>3</sup>, Matthew R. Scott<sup>63</sup>, Swapnil Rane<sup>18</sup>, Michael Rebsamen<sup>3</sup>, Hongliang Ren<sup>81</sup>, Xuhua Ren<sup>111</sup>, Mina Rezaei<sup>94</sup>, Pablo Ribalta Lorenzo<sup>71</sup>, Oliver Rippe<sup>31</sup>, Charlotte Robert<sup>42</sup>, Ahana Roy Choudhury<sup>46</sup>, Aaron S. Jackson<sup>37</sup>, B. S. Manjunath<sup>78</sup>, Mostafa Salem<sup>39</sup>, Joaquim Salvi<sup>39</sup>, Irina Sánchez<sup>98</sup>, Dawid Schellingerhout<sup>58</sup>, Zeina Shboul<sup>32</sup>, Haipeng Shen<sup>49</sup>, Dinggang Shen<sup>112</sup>, Varun Shenoy<sup>60</sup>, Feng Shi<sup>67</sup>, Hai Shu<sup>51</sup>, James Snyder<sup>40</sup>, Il Song Han<sup>62</sup>, Mehul Soni<sup>106</sup>, Jean Stawiaski<sup>77</sup>, Shashank Subramanian<sup>61</sup>, Li Sun<sup>29</sup>, Roger Sun<sup>41,42</sup>, Jiawei Sun<sup>45</sup>, Kay Sun<sup>59</sup>, Yu Sun<sup>68</sup>, Guoxia Sun<sup>114</sup>, Shuang Sun<sup>114</sup>, Moo Sung Park<sup>120</sup>, Laszlo Szilagy<sup>96</sup>, Sanjay Talbar<sup>19</sup>, Dacheng Tao<sup>25</sup>, Dacheng Tao<sup>89</sup>, Mohamed Tarek Khadir<sup>74</sup>, Siddhesh Thakur<sup>19</sup>, Guillaume Tochon<sup>28</sup>, Tuan Tran<sup>102</sup>, Kuan-Lun Tseng<sup>110</sup>, Vadim Turlapov<sup>84</sup>, Nicholas Tustison<sup>27</sup>, B. Uma Shankar<sup>35</sup>, Maria Vakalopoulou<sup>41,42</sup>, Sergi Valverde<sup>39</sup>, Rami Vanguri<sup>47,48</sup>, Evgeny Vasiliev<sup>84</sup>, Tom Vercauteren<sup>75,76</sup>, Lasitha Vidyaratne<sup>32</sup>, Ajeet Vivekanandan<sup>59</sup>, Guotai Wang<sup>75,76</sup>, Qian Wang<sup>111</sup>, Weichung Wang<sup>110</sup>, Ning Wen<sup>40</sup>, Xin Wen<sup>66</sup>, Leon Weninger<sup>31</sup>, Wolfgang Wick<sup>23</sup>, Shaocheng Wu<sup>107</sup>, Qiang Wu<sup>114,115</sup>, Yong Xia<sup>65</sup>, Yanwu Xu<sup>87</sup>, Xiaowen Xu<sup>114</sup>, Peiyuan Xu<sup>116</sup>, Tsai-Ling Yang<sup>44</sup>, Xiaoping Yang<sup>72</sup>, Hao-Yu Yang<sup>92,93</sup>, Junlin Yang<sup>92</sup>, Haojin Yang<sup>94</sup>, Hongdou Yao<sup>97</sup>, Brett Young-Moxon<sup>59</sup>, Xiangyu Yue<sup>60</sup>, Songtao Zhang<sup>29</sup>, Angela Zhang<sup>78</sup>, Kun Zhang<sup>89</sup>, Xuejie Zhang<sup>97</sup>, Lichi Zhang<sup>111</sup>, Xiaoyue Zhang<sup>117</sup>, Sicheng Zhao<sup>60</sup>, Yu Zhao<sup>64</sup>, Yefeng Zheng<sup>116</sup>, Liming Zhong<sup>52</sup>, Chenhong Zhou<sup>24</sup>, Xiaobing Zhou<sup>97</sup>, Hongtu Zhu<sup>50</sup>, Weiwei Zong<sup>40</sup>, Jayashree Kalpathy-Cramer<sup>122,123,†</sup>, Keyvan Farahani<sup>11,†,‡</sup>, Christos Davatzikos<sup>1,2,†,‡</sup>, Koen van Leemput<sup>8,122,123,124,†</sup>, Bjoern Menze<sup>8,64,126,†,\*</sup>

- <sup>1</sup> Center for Biomedical Image Computing and Analytics, University of Pennsylvania, USA
- <sup>2</sup> Department of Radiology, Hospital of the University of Pennsylvania, USA
- <sup>3</sup> Institute for Surgical Technology and Biomechanics, University of Bern, Switzerland
- <sup>4</sup> Center for MR-Research, University Children's Hospital Zurich, Switzerland
- <sup>5</sup> Support Centre for Advanced Neuroimaging Inselspital, Bern University Hospital, Switzerland
- <sup>6</sup> University Hospital of Zurich, Switzerland
- <sup>7</sup> Center for Clinical Epidemiology and Biostatistics, University of Pennsylvania, USA
- <sup>8</sup> Image-Based Biomedical Modeling Group, Technical University of Munich, Germany
- <sup>9</sup> Icahn School of Medicine, Mount Sinai Health System, USA
- <sup>10</sup> Leidos Biomedical Research, Inc., Frederick National Laboratory for Cancer Research, USA
- <sup>11</sup> Cancer Imaging Program, National Cancer Institute, National Institutes of Health, USA
- <sup>12</sup> Department of Neurology, The University of Alabama at Birmingham, USA
- <sup>13</sup> Department of Diagnostic Radiology, University of Texas MD Anderson Cancer Center, USA
- <sup>14</sup> Department of Psychology, Washington University in St. Louis, USA
- <sup>15</sup> Neuroimaging Informatics and Analysis Center, Washington University in St. Louis, USA
- <sup>16</sup> Department of Radiology, Washington University in St. Louis, USA
- <sup>17</sup> Institute of Radiology, University Hospital Rostock, Germany
- <sup>18</sup> Department of Radiodiagnosis, Tata Memorial Centre, Mumbai, India
- <sup>19</sup> Shri Guru Gobind Singhji Institute of Engineering and Technology, Nanded, India
- <sup>20</sup> NVIDIA, Santa Clara, USA
- <sup>21</sup> Division of Medical Image Computing, German Cancer Research Center (DKFZ), Heidelberg, Germany
- <sup>22</sup> Department of Neuroradiology, University of Heidelberg Medical Center, Heidelberg, Germany
- <sup>23</sup> Neurology Clinic, University of Heidelberg Medical Center, Heidelberg, Germany
- <sup>24</sup> School of Electronic & Information Engineering, South China University of Technology, Guangzhou, China
- <sup>25</sup> UBTECH Sydney AI Centre, SIT, FEIT, University of Sydney, Australia
- <sup>26</sup> Biomedical Engineering, University of Virginia, Charlottesville VA 22903, USA
- <sup>27</sup> Radiology & Medical Imaging, University of Virginia, Charlottesville VA 22903, USA
- <sup>28</sup> EPITA Research and Development Laboratory (LRDE), France
- <sup>29</sup> Southern University of Science and Technology, Shenzhen, China
- <sup>30</sup> Peking University, China
- <sup>31</sup> Institute of Imaging & Computer Vision, RWTH Aachen University, Aachen, Germany
- <sup>32</sup> Vision Lab, Electrical & Computer Engineering, Old Dominion University, USA
- <sup>33</sup> iTeam, Universitat Politècnica de València, Spain
- <sup>34</sup> Instituto de Física Corpuscular, Universitat de València, Consejo Superior de Investigaciones Científicas, Spain
- <sup>35</sup> Machine Intelligence Unit, Indian Statistical Institute, Kolkata, India
- <sup>36</sup> Department of CSE, University of Calcutta, Kolkata, India
- <sup>37</sup> Computer Vision Lab, School of Computer Science, University of Nottingham, UK
- <sup>38</sup> School of Biosciences, University of Nottingham, UK
- <sup>39</sup> Research Institute of Computer Vision and Robotics, University of Girona, Spain
- <sup>40</sup> Henry Ford Health System, USA
- <sup>41</sup> CVN, CentraleSupélec, Université Paris-Saclay, France
- <sup>42</sup> Gustave Roussy Institute, France
- <sup>43</sup> TheraPanacea, France
- <sup>44</sup> Department of Electrical Engineering, National Taiwan University of Science & Technology, Taiwan
- <sup>45</sup> Dept. of Biomedical Engineering, School of Control Science & Engineering, Shandong University, China
- <sup>46</sup> Department of Computer Science, Florida State University, USA
- <sup>47</sup> Department of Radiology, Columbia University Medical Center, USA

- <sup>48</sup> Data Science Institute, Columbia University, USA
- <sup>49</sup> Faculty of Business and Economics, The University of Hong Kong, Hong Kong
- <sup>50</sup> Department of Biostatistics, University of North Carolina at Chapel Hill, USA
- <sup>51</sup> Department of Biostatistics, University of Texas, MD Anderson Cancer Center, USA
- <sup>52</sup> Guangdong Provincial Key Laboratory of Medical Image Processing, School of Biomedical Engineering, Southern Medical University, Guangzhou, China
- <sup>53</sup> Research Center for Brain-inspired Intelligence, Institute of Automation, Chinese Academy of Sciences, China
- <sup>54</sup> University of Chinese Academy of Sciences, China
- <sup>55</sup> Center for Excellence in Brain Science and Intelligence Technology, Chinese Academy of Sciences, China
- <sup>56</sup> Afeka Academic College of Engineering, Tel Aviv, Israel
- <sup>57</sup> Department of Imaging Physics, University of Texas MD Anderson Cancer Center, USA
- <sup>58</sup> Department of Cancer Systems Imaging and Diagnostic Radiology, University of Texas MD Anderson Cancer Center, USA
- <sup>59</sup> HealthMyne, USA
- <sup>60</sup> University of California, Berkeley, USA
- <sup>61</sup> University of Texas, Austin, USA
- <sup>62</sup> Odiga London, UK
- <sup>63</sup> Malong Tehnologies, China
- <sup>64</sup> Department of Computer Science, Technical University of Munich, Germany
- <sup>65</sup> Computer Science & Engineering, Northwestern Polytechnical University, University of Xi'an, China
- <sup>66</sup> The First Affiliated Hospital of Xi'an Jiao Tong University, People's Republic of China, China
- <sup>67</sup> Shanghai United Imaging Intelligence Co., Ltd, Shanghai, China
- <sup>68</sup> School of Biomedical Engineering, Southeast University, Nanjing, China
- <sup>69</sup> Harvard University, USA
- <sup>70</sup> Future Processing, Poland
- <sup>71</sup> Silesian University of Technology, Gliwice, Poland
- <sup>72</sup> Department of Mathematics, Nanjing University of Science and Technology, China
- <sup>73</sup> LMCS Laboratory, National Higher School of Computer Sciences (ESI), Algeria
- <sup>74</sup> LabGed Laboratory, Dept. of Computer Sciences, University Badji-Mokhtar of Annaba, Algeria
- <sup>75</sup> School of Biomedical Engineering and Imaging Sciences, King's College London, UK
- <sup>76</sup> Wellcome / EPSRC Centre for Interventional and Surgical Sciences, University College London, UK
- <sup>77</sup> Stryker Corporation, Navigation. Freiburg im Breisgau, Germany.
- <sup>78</sup> Vision Research Lab, University of California, USA
- <sup>79</sup> UC Irvine Health, University of California, USA
- <sup>80</sup> Graduate School for Integrative Sciences and Engineering, National University of Singapore, Singapore
- <sup>81</sup> Department of Biomedical Engineering, National University of Singapore, Singapore
- <sup>82</sup> Dept. of Instrumentation and Control Engineering, National Institute of Technology, Tiruchirappalli, India
- <sup>83</sup> Intel, Nizhny Novgorod, Russian Federation
- <sup>84</sup> Lobachevsky State University, Russian Federation
- <sup>85</sup> Technological Institute of Irapuato, Information Technologies Laboratory, Mexico
- <sup>86</sup> College of Engineering, Mathematics and Physical Sciences, University of Exeter, UK
- <sup>87</sup> Department of Biomedical Informatics, University of Pittsburgh, USA
- <sup>88</sup> Philosophy Department, Carnegie Mellon University, USA
- <sup>89</sup> UBTECH Sydney AI Centre, SIT, FEIT, The University of Sydney, Australia
- <sup>90</sup> University of Washington, USA
- <sup>91</sup> Centre for Intelligent Machines (CIM), McGill University, Canada
- <sup>92</sup> Yale University, USA

- <sup>93</sup> Cura Cloud Cooperation, USA
- <sup>94</sup> Hasso Plattner Institute, Germany
- <sup>95</sup> Department of Computer Science, University of Medicine, Pharmacy, Sciences and Technology, Romania
- <sup>96</sup> Department of Electrical Engineering, Sapiientia Hungarian University of Transylvania, Romania
- <sup>97</sup> School of Information Science and Engineering, Yunnan University, P.R.China
- <sup>98</sup> QMENTA, USA
- <sup>99</sup> Computer Vision Center, Universitat Autònoma de Barcelona, Spain
- <sup>100</sup> SIMBIOSys, Universitat Pompeu Fabra, Spain
- <sup>101</sup> University Clinic for Radio-oncology, Bern University Hospital, Switzerland
- <sup>102</sup> Faculty of Math and Computer Science, University of Science, Vietnam National University, Vietnam
- <sup>103</sup> Department of Computer Science, Sai Gon University, Vietnam
- <sup>104</sup> INESC-ID, Portugal
- <sup>105</sup> Instituto Superior Técnico, Portugal
- <sup>106</sup> Indian Institute of Technology Madras, India
- <sup>107</sup> University of Michigan, USA
- <sup>108</sup> Indian Institute of Technology Roorkee, India
- <sup>109</sup> Tianjin University, China
- <sup>110</sup> National Taiwan University, Taiwan
- <sup>111</sup> School of Biomedical Engineering, Shanghai Jiao Tong University, China
- <sup>112</sup> Department of Radiology and BRIC, University of North Carolina at Chapel Hill, USA
- <sup>113</sup> Department of biological science and medical engineering, Beihang University, China
- <sup>114</sup> School of Information Science and Engineering, Shandong University, China
- <sup>115</sup> Institute of Brain and Brain-Inspired Science, Shandong University, China
- <sup>116</sup> Tencent Youtu Lab, China
- <sup>117</sup> QED Technologies. Co., Ltd, China
- <sup>118</sup> Beihang University, China
- <sup>119</sup> Beijing University of Posts and Telecommunications University, China
- <sup>120</sup> Deepnoid, South Korea
- <sup>121</sup> Department of Neurosurgery, Mount Sinai Health System, USA
- <sup>122</sup> Athinoula A Martinos Center for Biomedical Imaging, Massachusetts General Hospital, USA
- <sup>123</sup> Department of Radiology, Harvard Medical School, Harvard University, USA
- <sup>124</sup> Department of Applied Mathematics and Computer Science, Technical University of Denmark
- <sup>125</sup> Department of Neuroradiology, Technical University of Munich, Germany
- <sup>126</sup> Institute for Biomedical Engineering, Technical University of Munich, Germany

<sup>†</sup> People involved in the organization of the challenge

<sup>‡</sup> People contributing data from their institutions

\* Corresponding author

< s.bakas@uphs.upenn.edu, bjoern.menze@tum.de >

## **Abstract**

Gliomas are the most common primary brain malignancies, with different degrees of aggressiveness, variable prognosis and various heterogeneous histologic sub-regions, i.e., peritumoral edematous/invaded tissue, necrotic core, active and non-enhancing core. This intrinsic heterogeneity is also portrayed in their radio-phenotype, as their sub-regions are depicted by varying intensity profiles disseminated across multi-parametric magnetic resonance imaging (mpMRI) scans, reflecting varying biological properties. Their heterogeneous shape, extent, and location are some of the factors that make these tumors difficult to resect, and in some cases inoperable. The amount of resected tumor is a factor also considered in longitudinal scans, when evaluating the apparent tumor for potential diagnosis of progression. Furthermore, there is mounting evidence that accurate segmentation of the various tumor sub-regions can offer the basis for quantitative image analysis towards prediction of patient overall survival. This study assesses the state-of-the-art machine learning (ML) methods used for brain tumor image analysis in mpMRI scans, during the last seven instances of the International Brain Tumor Segmentation (BraTS) challenge, i.e. 2012-2018. Specifically, we focus on i) evaluating segmentations of the various glioma sub-regions in pre-operative mpMRI scans, ii) assessing potential tumor progression by virtue of longitudinal growth of tumor sub-regions, beyond use of the RECIST criteria, and iii) predicting the overall survival from pre-operative mpMRI scans of patients that undergone gross total resection. Finally, we investigate the challenge of identifying the best ML algorithms for each of these tasks, considering that apart from being diverse on each instance of the challenge, the multi-institutional mpMRI BraTS dataset has also been a continuously evolving/growing dataset.

## **Keywords**

BraTS, challenge, brain, tumor, segmentation, machine learning, glioma, glioblastoma, radiomics, survival, progression, RECIST

# 1. Introduction

## 1.1. Scope

The Brain Tumor segmentation (BraTS) challenge focuses on the evaluation of state-of-the-art methods for the segmentation of brain tumors in multi-parametric magnetic resonance imaging (mpMRI) scans. Its primary role since its inception has been two-fold: a) a publicly available dataset and b) a community benchmark [1-4]. BraTS utilizes multi-institutional pre-operative mpMRI scans and focuses on the segmentation of intrinsically heterogeneous (in appearance, shape, and histology) brain tumors, namely gliomas. Furthermore, to pinpoint the clinical relevance of this segmentation task, BraTS 2018 also focuses on the prediction of patient overall survival, via integrative analyses of radiomic features and machine learning (ML) algorithms.

## 1.2. Clinical Relevance

Gliomas are the most common primary brain malignancies, with different degrees of aggressiveness, variable prognosis and various heterogeneous histological sub-regions, i.e., peritumoral edematous/invaded tissue, necrotic core, active and non-enhancing core. This intrinsic heterogeneity of gliomas is also portrayed in their imaging phenotype (appearance and shape), as their sub-regions are described by varying intensity profiles disseminated across mpMRI scans, reflecting varying tumor biological properties. Due to this highly heterogeneous appearance and shape, segmentation of brain tumors in multimodal MRI scans is one of the most challenging tasks in medical image analysis.

## 1.3. Before the BraTS era

There has been a growing body of literature on computational algorithms addressing this important task (Fig.1). Unfortunately, open manually-annotated datasets for designing and testing these algorithms are not currently available, and private datasets differ so widely that it is hard to compare the different segmentation strategies that have been reported so far. Critical factors leading to these differences include, but not limited to, i) the imaging modalities employed, ii) the type of the tumor (glioblastoma or lower grade glioma, primary or secondary tumors, solid or infiltratively growing), and iii) the state of disease (images may not only be acquired prior to treatment, but also post-operatively and therefore show radiotherapy effects and surgically-imposed cavities). Towards this end, BraTS is making available a large dataset of mpMRI [1-4], with accompanying delineations of the relevant tumor sub-regions (Fig.2). The exact mpMRI data consists of a) a native T1-weighted scan (T1), b) a post-contrast T1-weighted scan (T1Gd), c) a native T2-weighted scan (T2), and d) a T2 Fluid Attenuated Inversion Recovery (T2-FLAIR) scan.

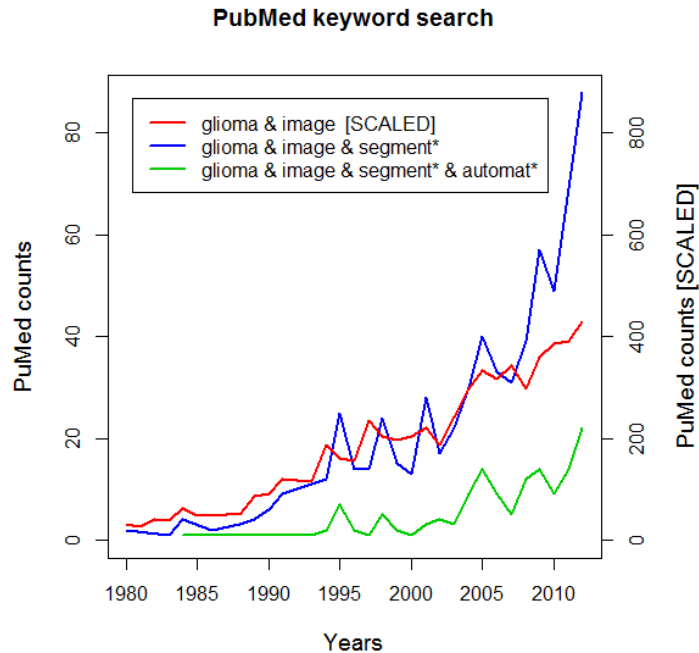


Figure 1. Search on PubMed in 2012 showing related growing body of literature. Figure taken from [1].

#### 1.4. BraTS 2017 and 2018

The last two instances of BraTS (i.e., 2017 and 2018) were focused on both the segmentation of tumor sub-structures, and the prediction of overall survival of patients diagnosed with primary *de novo* glioblastoma (GBM).

For the segmentation of gliomas in pre-operative mpMRI scans, the participants were called to address this task by using the provided clinically-acquired training data to develop automated methods and produce segmentation labels of the different glioma sub-regions.

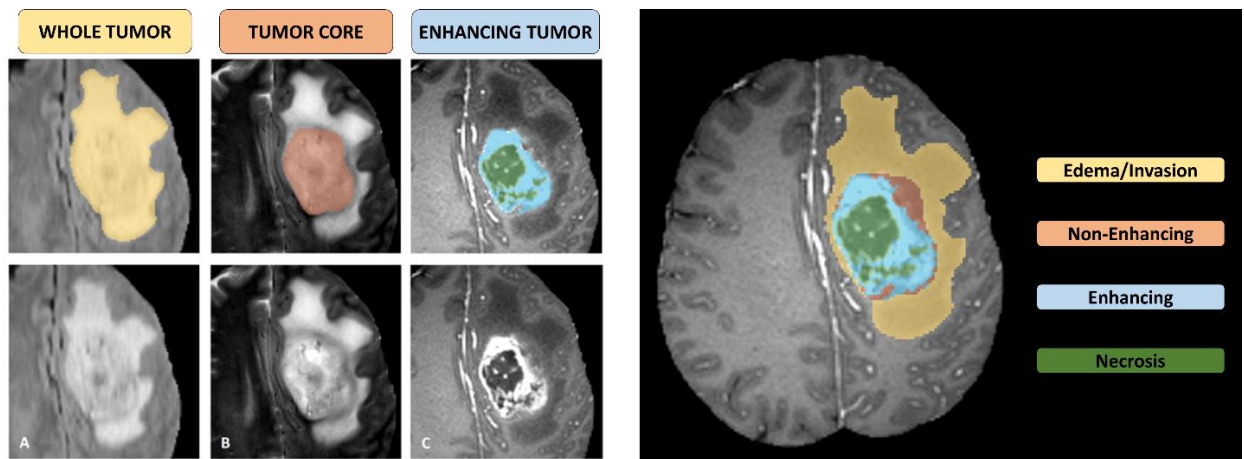


Figure 2. Glioma sub-regions. The image patches show from left to right: the whole tumor (yellow) visible in T2-FLAIR (A), the tumor core (red) visible in T2 (B), the active tumor structures (light blue) visible in T1Gd, surrounding the cystic/necrotic components of the core (green) (C). The segmentations are combined to generate the final labels of the tumor sub-regions (D): ED (yellow), NET (red), NCR cores (green), AT (blue). Figure taken from [1].

For the task of patient overall survival (OS) prediction from pre-operative mpMRI scans, once the participants produce their segmentation labels in the pre-operative scans, they were called to use these labels in combination with the provided mpMRI data to extract imaging/radiomic features that they consider appropriate [5], and analyze them through ML algorithms, to predict patient OS (Fig.3). The participants do not need to be limited to volumetric parameters, but can also consider intensity, morphologic, histogram-based, and textural features, as well as spatial information, and glioma diffusion properties extracted from glioma growth models.

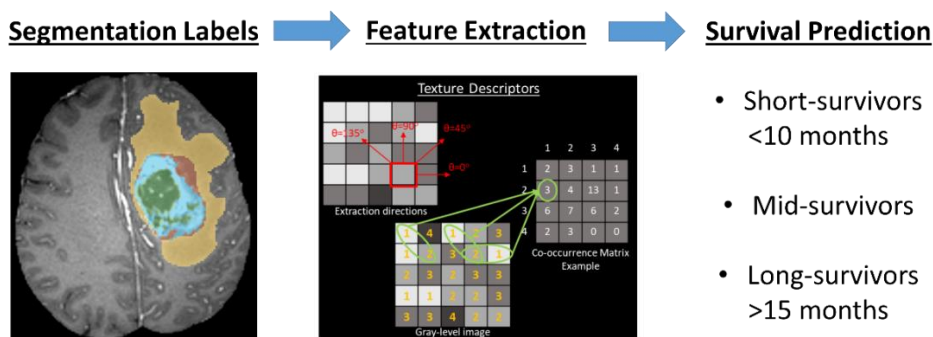


Figure 3. Illustrative pipeline example for predicting patient overall survival.

## 2. Materials & Methods

### 2.1. BraTS Annotations and Structures

All the imaging datasets have been segmented manually, by one to four raters, following the same annotation protocol, and their ground truth annotations were approved by experienced neuro-radiologists. The tumor sub-regions considered for evaluation are: 1) the "active tumor" (AT), 2) the "tumor core" (TC), and 3) the "whole tumor" (WT) (Fig.2). The AT is described by areas that show hyper-intensity in T1Gd when compared to T1, but also when compared to "healthy" white matter in T1Gd. The TC describes the bulk of the tumor, which is what is typically resected. The TC entails the AT, as well as the necrotic (fluid-filled) and the non-enhancing (solid) parts of the tumor. The appearance of the necrotic (NCR) and the non-enhancing (NET) tumor core is typically hypo-intense in T1-Gd when compared to T1. The WT describes the complete extent of the disease, as it entails the TC and the peritumoral edematous/invaded tissue (ED), which is typically depicted by hyper-intense signal in T2-FLAIR. The labels in the BraTS provided data are: 1 for NCR & NET, 2 for ED, 4 for AT, and 0 for everything else.

The ground truth annotations were only approved by domain experts whereas they are actually created by multiple experts. Although a very specific annotation protocol was provided to each data contributing institution, slightly different annotation styles were noted for the various raters involved in the process. Therefore, all final labels included in the BraTS dataset were also further reviewed for consistency and compliance with the annotation protocol by a single board-certified neuro-radiologist with more than 15 years of experience.

## 2.2. The BraTS Data Since its Inception

The mpMRI scans made publicly available through the BraTS initiative, describe T1, T1Gd, T2, and T2-FLAIR volumes, acquired with different clinical protocols and various scanners from multiple institutions, mentioned as data contributors in the acknowledgements section. The provided data are distributed after their harmonization, following standardization pre-processing without affecting the apparent information in the images. Specifically, the pre-processing routines applied in all the BraTS mpMRI scans include co-registration to the same anatomical template [6], interpolation to a uniform isotropic resolution (1 mm<sup>3</sup>), and skull-stripping.

### 2.2.1. Continuously Growing Publicly Available Dataset

The BraTS dataset has evolved over the years (2012-2018) with a continuously increasing number of patient cases, as well as through an improvement of the data split used for algorithmic development and evaluation.

The first two instances of BraTS (2012-2013) comprised a training and a testing dataset of 35 and 15 mpMRI patient scans, respectively. The results and findings of these two first editions, were summarized in [1], which to date is the most popular and downloaded paper of the IEEE TMI journal since its publication, and reflects the interest of the scientific research community in the BraTS initiative as a publicly available dataset and a community benchmark.

The subsequent three instances of BraTS (2014-2016) received a substantial dataset increase in two waves and also included longitudinal mpMRI scans. The first wave of increase came in during 2014-2015 primarily from contributions of The Cancer Imaging Archive (TCIA) repository [7] and then Heidelberg University, and the second wave of increase happened in 2016 with contributions from the Center for Biomedical Image Computing and Analytics (CBICA) at the University of Pennsylvania (UPenn). In addition, stemming from the analysis of the BraTS 2012-2013 results [1], BraTS 2014-2016 employed ground-truth data created by label fusion of top-performing approaches.

In 2017, thanks to additional contributions to the BraTS dataset, from CBICA@UPenn and the University of Alabama in Birmingham (UAB), a validation set was included to facilitate algorithm fine-tuning following a ML paradigm of training, validation, and testing datasets. Notably, in 2017 the number of cases was doubled with respect to the previous year, amounting to 477 cases, which was further increased in 2018 with 542 cases, thanks to contributions from MD Anderson Cancer Center in Texas, the Washington University School of Medicine in St. Louis, and the Tata Memorial Center in India.

### 2.2.2. Focus Beyond Segmentation

BraTS, as indicated by its acronym definition, has primarily focused on the segmentation to brain tumor sub-regions. However, after its first instances (2012-2013), its potential clinical relevance became apparent.

BraTS was introduced with secondary tasks, where the results of the brain tumor segmentation algorithms are used towards promoting further analysis and accelerating discovery. From a clinical perspective these secondary tasks featured in the BraTS challenge can be crucial towards fostering the development of algorithms capable of addressing clinical requirements in a more reliable manner than the current clinical practice. Specifically, to pinpoint the clinical relevance of the segmentation task, in the BraTS instances of 2014-2016, longitudinal scans were included in the publicly available dataset, to evaluate the ability and

potential of automated tumor volumetry in assessing disease progression. Along the same lines of research, in the last two instances of BraTS (2017-2018), clinical data of patient age, overall survival, and resection status were included, to facilitate the secondary task of predicting patient overall survival via integrative analyses of radiomic features and ML algorithms.

Table 1. Summarizing the distribution of the BraTS data across the training, validation, and testing sets, since the inception the of BraTS initiative, together with the focused tasks of its BraTS instance.

BraTS Instance	Training data	Validation data	Testing data	Tasks	Type of data
2012	35	N/A	15	Segmentation	Pre-operative only
2013	35	N/A	25	Segmentation	Pre-operative only
2014	200	N/A	38	Segmentation, Assessment of disease progression	Longitudinal
2015	200	N/A	53	Segmentation, Assessment of disease progression	Longitudinal
2016	200	N/A	191	Segmentation, Assessment of disease progression	Longitudinal
2017	285	46	146	Segmentation, Prediction of patient overall survival	Pre-operative only
2018	285	66	191	Segmentation, Prediction of patient overall survival	Pre-operative only

### 2.2.3. The Latest BraTS Data

The datasets used in BraTS 2017 and 2018 have been updated (since BraTS 2016), with more routine clinically-acquired 3T mpMRI scans and all the ground truth labels have been evaluated, and manually-revised when needed, by expert board-certified neuroradiologists. Ample multi-institutional (n=19) routine clinically-acquired pre-operative mpMRI scans of GBM/HGG and LGG, with pathologically confirmed diagnosis and available OS, were provided as the training, validation and testing data.

The data provided since BraTS 2017 differs significantly from the data provided during the previous BraTS challenges (i.e., 2016 and backwards). Specifically, since BraTS 2017, expert neuroradiologists have radiologically assessed the complete original TCIA glioma collections (i.e., TCGA-GBM, n=262 [8] and TCGA-LGG, n=199 [9]) and categorized each scan as pre-operative or post-operative. Subsequently, all the pre-operative TCIA scans (i.e., 135 GBM and 108 LGG) were annotated by experts for the various sub-regions and included in the BraTS datasets [2-4].

### 2.2.4. Data Availability

As one of the main objectives of the BraTS initiative is to provide an open source repository for continuous development of algorithms, the data of BraTS 2012-2016 has been made available through the Swiss Medical Image Repository (SMIR – [www.smir.ch](http://www.smir.ch)), and the data of BraTS 2017-2018 through the Image Processing Portal of the CBICA@UPenn (IPP – [ipp.cbica.upenn.edu](http://ipp.cbica.upenn.edu)). Both platforms feature downloading of datasets, as well as the automatic evaluation of the results submitted by participants.

#### **2.4. The Ranking Scheme for the Segmentation Task (BraTS 2017-2018)**

The ranking scheme followed during the BraTS 2017 and 2018 comprised the ranking of each team relative to its competitors for each of the testing subjects, for each evaluated region (i.e., AT, TC, WT), and for each measure (i.e., Dice and Hausdorff (95%)). For example, in BraTS 2018, each team was ranked for 191 subjects, for 3 regions, and for 2 metrics, which resulted in 1146 individual rankings. The final ranking score was then calculated by averaging across all these individual rankings and then normalized by dividing by the number of teams. This ranking scheme has also been adopted in other challenges with satisfactory results, such as the Ischemic Stroke Lesion Segmentation (ISLES - <http://www.isles-challenge.org/>) challenge [10, 11].

#### **2.5. Prediction of Patient Overall Survival (BraTS 2017-2018)**

We identified 346 GBM patients with overall survival (OS), age, and resection status information. 164 of them had undergone surgery with gross total resection (GTR) status. The distributions of OS of GBM patients across the training, validation and testing datasets were matched (Fig.X). The patients were divided in three groups of survival comprising long-survivors (who survived more than 15 months), short-survivors (who survived less than 10 months), and mid-survivors (who survived between 10 and 15 months). These thresholds were derived after statistical consideration of the survival distributions across the complete dataset. Specifically, we chose these thresholds based on equal quantiles from the median OS (approximately 12.5 months) to avoid potential bias towards one of the survival groups (short- vs long-survivors) and while considering that discrimination of groups should be clinically meaningful. The median OS of the described cohorts is not significantly different from the median OS of GBM patients in several randomized Phase III trials, noting that our cohort consists of unselected patients rather than those eligible for such trials [12, 13].

The population of patients with available OS information was randomly and proportionally divided into the training, validation and testing sets. This process formed a) the training set, consisting of 163 cases (59 with GTR), b) the validation set, consisting of 53 cases (28 with GTR), and c) the testing set, consisting of 130 cases (77 with GTR). Figure 4 shows the distribution of patient cases for the task of the OS prediction.

Participating teams were requested to submit OS prediction results in days for each patient with GTR. The evaluation system then automatically classified these into short-, intermediate-, and long-survivors.

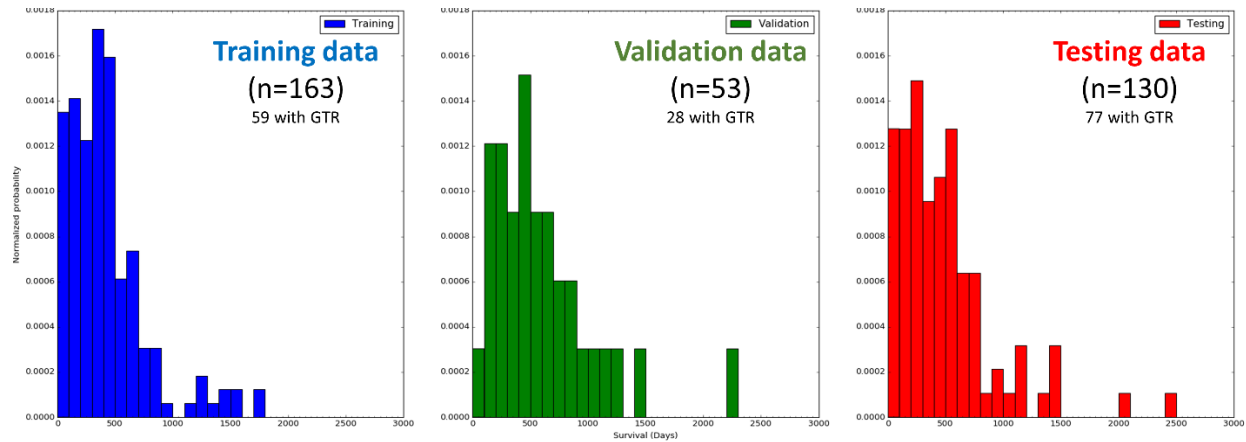


Figure 4. The overall survival distribution of patients across the training, validation, and testing sets of BraTS.

## 2.6. Evaluation Framework

For consistency purposes both in BraTS 2017 & 2018 challenges, two reference standards were used for the two tasks of the challenge: 1) manual segmentation labels of tumor sub-regions, and 2) clinical data of OS.

The introduction of the validation set since BraTS 2017 allows participants to obtain preliminary results in unseen data, in addition to their cross-validated results on the training data. The ground truth of the validation data was never provided to the participants. Finally, all participants were presented with the same test data, for a limited controlled time-window (48h), before the participants are required to submit their final results for quantitative evaluation and their ranking.

For the segmentation task, and for consistency with the configuration of the previous BraTS challenges, the "Dice score" and the "Hausdorff distance" were used. Expanding upon this evaluation scheme, the metrics of "Sensitivity" and "Specificity" were also used, allowing to determine potential over- or under-segmentations of the tumor sub-regions by participating methods. Since the BraTS 2012-2013 were subsets of the BraTS 2018 test data, performance comparison on the 2012-2013 data will allow for a direct evaluation against the performances reported in [1].

For the task of survival prediction, two evaluation schemes are considered. First, for ranking the participating teams, evaluation will be based on the classification of subjects as long-, intermediate-, and short-survivors. Predictions of the participating teams will be assessed based on classification accuracy (i.e. the number of correctly classified patients) with respect to this grouping. Note that participants are expected to provide predicted survival status only for subjects with resection status of GTR (i.e., Gross Total Resection). In addition, a pairwise error analysis between the predicted and actual survival in days was conducted and the results were shared with the participants, to allow the evaluation of their method for outliers. This analysis was done using the metrics of Mean-Square Error (MSE), median square error (medianSE), standard deviation of the square errors (stdSE), and the spearman correlation coefficient (spearmanR).

### 3. Results

#### 3.1. BraTS 2012-2013

To emphasize the most interesting results of our previously published analyses summarizing BraTS 2012 and BraTS 2013 [1], we focus into two main points (Fig.5). First, we note that even though most of the individual automated segmentation methods performed well, they did not outperform the inter-rater agreement, across expert clinicians, who have been trained for years to identify regions of infiltration and distinguish them from healthy brain. Secondly, the fusion of segmentation labels from top-ranked algorithms outperformed all individual methods and was comparable to inter-rater agreement. More specifically, while we observe that individual automated segmentation methods do not necessarily rank equally well in the different tumor segmentation tasks and under all metrics (i.e., when evaluating WT, TC, and AT segmentation, with respect to Dice score and Hausdorff distance), we note that the fused segmentation labels do consistently rank first in all tasks and both metrics. This suggests that ensembles of fused segmentation algorithms may be the favorable approach when translating tumor segmentation methods into clinical practice.

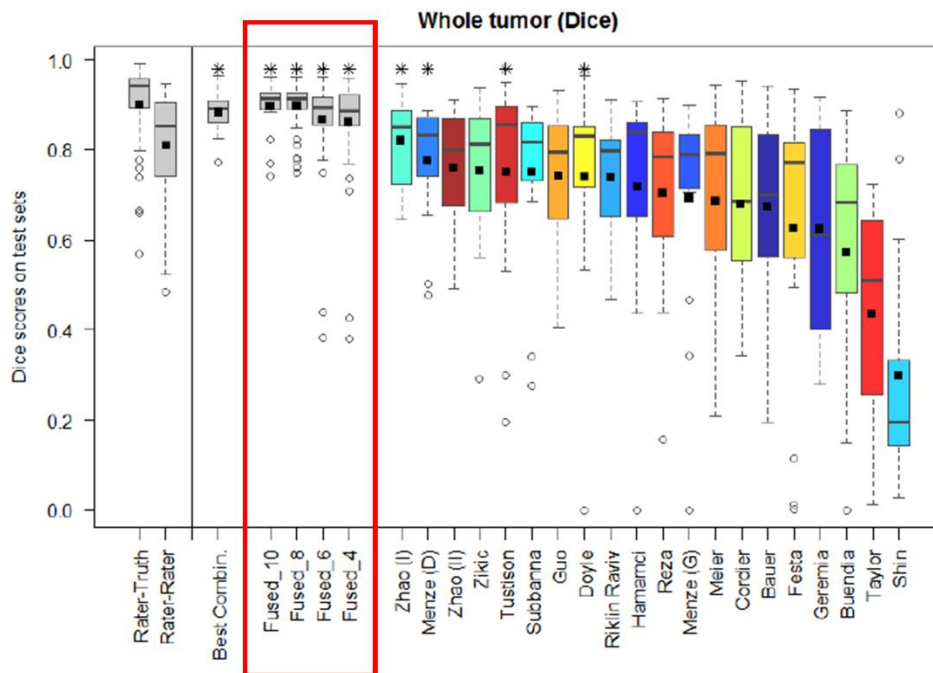


Figure 5. Summary results of the BraTS 2012-2013. Label fusion (red outline) out-performs all individual methods and the inter-rater agreement. Figure adopted from [1].

#### 3.2. BraTS 2018 (Testing Phase)

The BraTS 2018 results for the segmentation of the AT (Suppl.Fig.1) show a very marked skewness in the distribution of Dice metrics, as seen in the average and median values (crosses and vertical lines on each boxplot). These results illustrate the tendency of most methods to perform relatively well, in terms of

median Dice (Median Dice for top 54/63 teams: [0.74-0.85]), but also the difference in levels of robustness as the average Dice is affected by increasing number of outliers in the results (Average Dice of same 54/63 teams: [0.61-0.77]). Segmentation results of the TC (Suppl.Fig.2) presents a similar pattern, with the results of the AT, across teams. Similarly with observations from previous BraTS instances [1], the top positions are not systematically taken by the same teams, reflecting the added value of fusing segmentation labels from different approaches. In comparison to the AT, segmentation of the TC seems in general to be more robust (i.e., median inter-quantile range (IQR) for Dice of same 54/63 teams, for TC is 0.16, vs. 0.18 for the AT). It is worth mentioning though that the Dice metric is more sensitive to error of the AT, due to its typically much smaller volume. As also noted in previous instances of BraTS, the segmentation of the WT (Suppl.Fig.3) represents the most robust and accurate segmentation results of the three evaluated tumor compartments (i.e., AT, TC, WT), with a median Dice coefficient of 0.9 for most of the participating teams.

The 95% Hausdorff distance metric is used to characterize the levels of robustness of the automated results. Supplementary Figures 4 through 6 show the Hausdorff metric values for the three evaluated tumor compartments for all teams. Overall, the results for the AT seems to be the most robust for all three tumor labels (median IQR of 1.9 for the same 54/63 teams), followed by the results for the WT and that for the TC (IQR of 4.0 and 5.4 for the same 54/63 teams, respectively).

At the patient-wise ranking of the participating teams (Fig.6) the distribution follows more closely a gradual improvement of the ranked approaches. Worth noting is that the variability of the ranking of approaches at the case level does not dramatically change across teams, indicating no particular dominance of a method over the others. However, performing a pairwise comparison for significant differences based on 100,000 permutations shows statistically significant performances across teams. Specifically, the statistical evaluation of the top-ranked teams revealed that the first team was statistically better from the second ( $p$ -value=0.02), whereas the second team was not statistically better than the third ( $p$ =0.06) and the fourth ( $p$ =0.07), but only from the fifth ( $p$ =0.01). This justified the decision of a tie in the third rank.

Results of the survival task are shown in Fig.7. Overall, the top-5 approaches obtained an accuracy around 0.6, while the rest of teams obtained an accuracy in the range of [0.15-0.55]. We should clarify that the random choice should be considered the 0.33 since this is a 3-class classification.

The final top-performing participating teams positioned in ranks 1-3 are shown in Table 2.

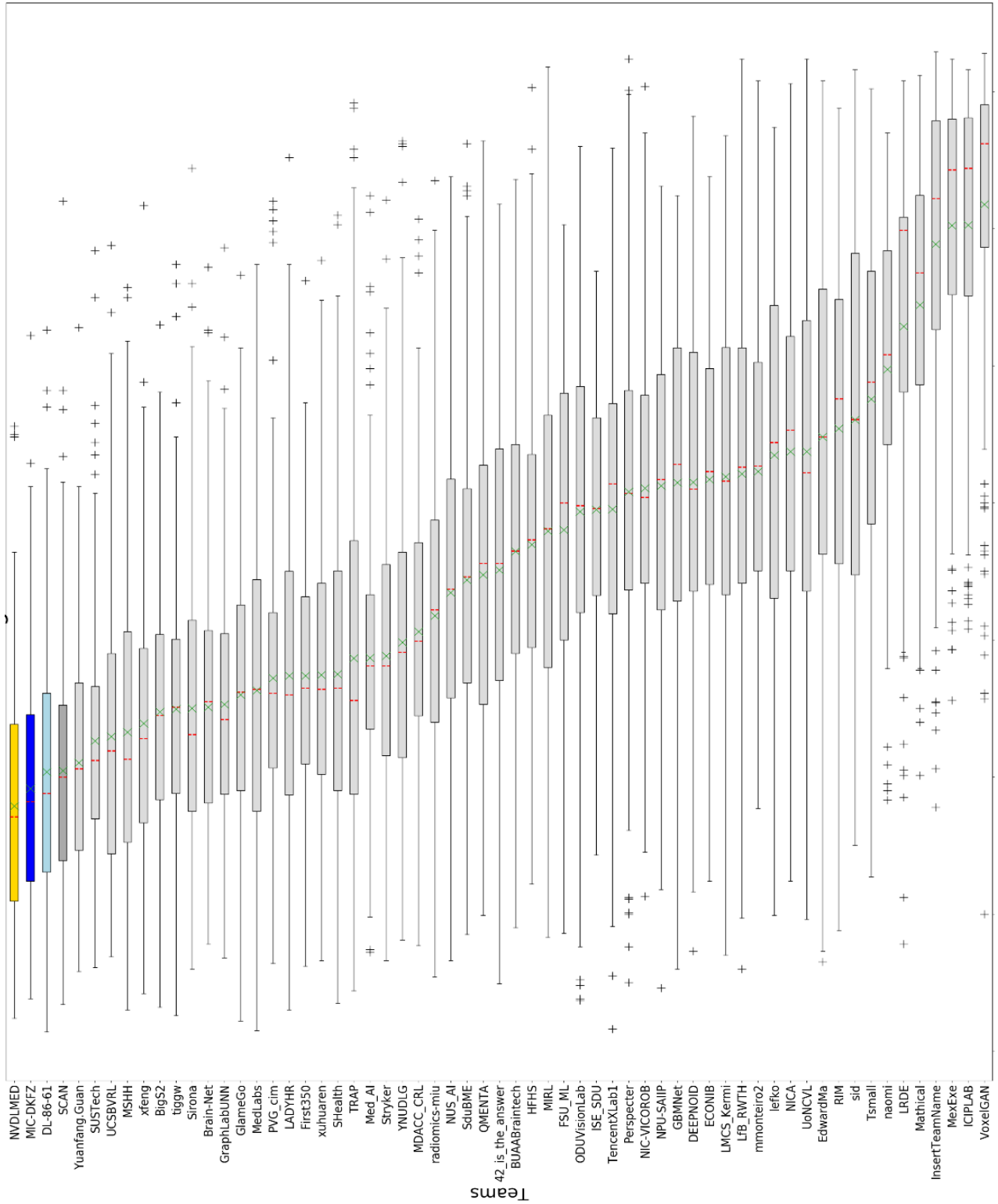


Figure 6. BrATS 2018 Ranking of all Participating Teams in Segmentation Task. (smaller values are higher ranks)

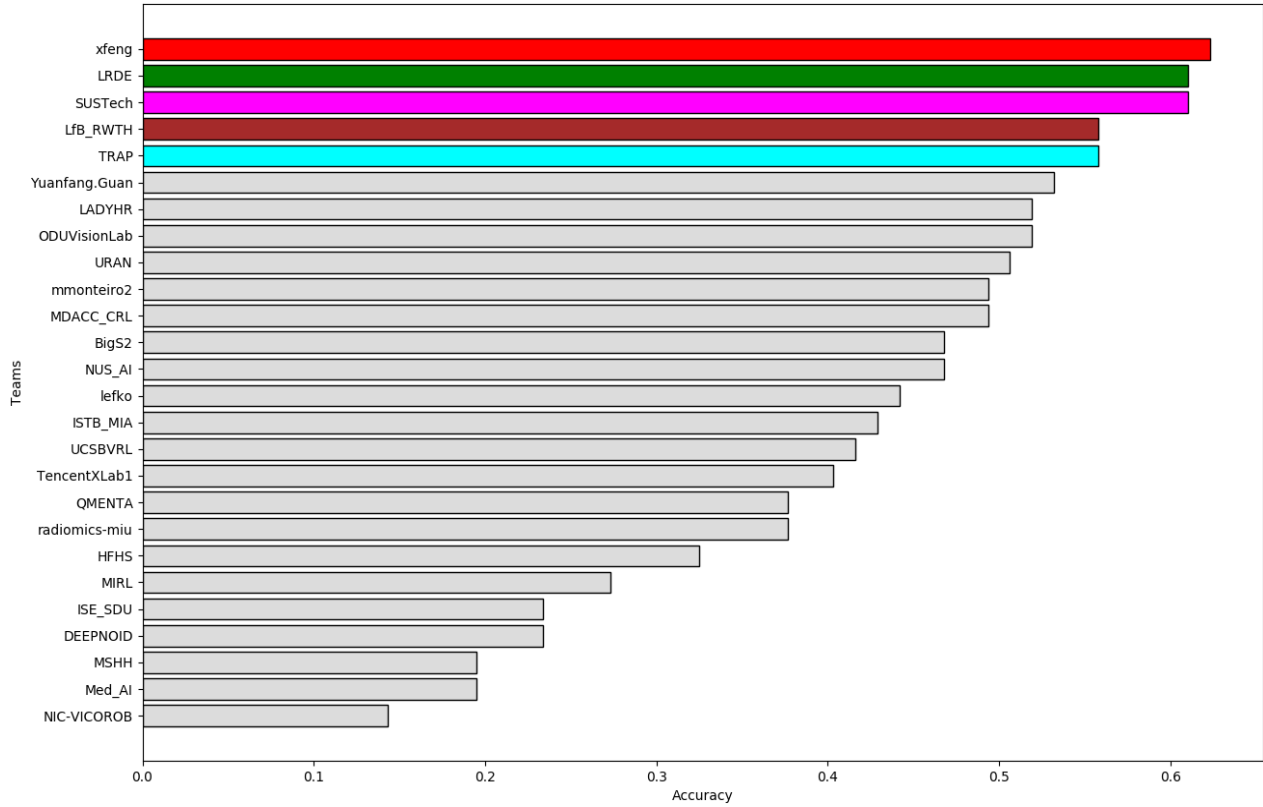


Figure 7. BraTS 2018 Ranking of all Participating Teams in Survival Task. (larger values are better)

Table 2. Top-ranked participating teams in BraTS 2018 for both the segmentation and the survival prediction tasks.

Task	Rank	Team	First Author	Institution
SEGMENTATION	1	NVDLMED	Andriy Myronenko	NVIDIA, Santa Clara, USA
	2	MIC-DKFZ	Fabian Isensee	Division of Medical Image Computing, German Cancer Research Center (DKFZ), Heidelberg, Germany
	3 (tie)	SCAN	Richard McKinley	Support Centre for Advanced Neuroimaging Inselspital, Bern University Hospital, Switzerland
	3 (tie)	DL_86_81	Chenhong Zhou	School of Electronic & Information Engineering, South China University of Technology, China
SURVIVAL PREDICTION	1	xfeng	Xue Feng	Biomedical Engineering, University of Virginia, USA
	2 (tie)	LRDE	Élodie Puybareau	EPITA Research and Development Laboratory, France
	2 (tie)	SUSTech	Li Sun	Southern University of Science & Technology, China
	3 (tie)	TRAP	Ujjwal Baid	Shri Guru Gobind Singhji Institute of Engineering and Technology, India
	3 (tie)	LfB_RWTH	Leon Weninger	Institute of Imaging & Computer Vision, RWTH Aachen University, Germany

## 4. Discussion

### 4.1. Performance of Automated Segmentation Methods

While the accuracy of individual automated segmentation methods has improved, we note that their level of robustness is still inferior to expert performance, i.e., inter-rater agreement. This robustness is expected to be continuously improving as the training set increases in size, in virtue of capturing and describing more diverse patient populations, along with improved training schemes and ML architectures. Beyond these speculative expectations, the results of our quantitative analyses support that the fusion of segmentation labels from various individual automated methods shows robustness superior to the ground truth inter-rater agreement (provided by clinical experts), in terms of both accuracy and consistency across subjects. However, proposed strategies to ensemble several models correspond to one practical way to reduce outliers and improve the precision of automated segmentation systems, by means of consensus segmentation across different models.. We consider future research essential, in order to improve the robustness of individual approaches by increasing the ability of segmentation systems to handle confounding effects typically seen in images acquired using routine clinical workflows. Related to BraTS such effects include, but are not limited to, a) the presence of blood products, b) “air-pockets”/resection cavities in post-operative scans, c) better differentiation (or handling) of non-GBM entities, and d) improved performance for low-grade gliomas, featuring diffuse boundaries, especially while considering cases without AT sub-regions, and e) high sensitivity to effectively detect and assess their slow progression.

### 4.2. BraTS Ranking Schema

The BraTS challenge recently adopted a case-wise ranking schema, which enables a more clinically-relevant evaluation of participating teams, as it considers the complexity of patient cases that can vary significantly. Furthermore, the additional featured evaluation of statistical significance of differences across algorithmic results, also enables the evaluation of results across different instances of the BraTS challenge, which in turns enables a thorough analysis of the improvement attained over the last seven years of the BraTS initiative.

### 4.3. Beyond Segmentation

Importantly, two more clinically-relevant tasks/sub-challenges have been complementarily added in the BraTS initiative during these past seven years, aiming at emphasizing the clinical relevance of the brain tumor segmentation task. Both these clinically-relevant tasks promote the natural utilization of segmentation labels to answer clinical questions, address clinical requirements, and potentially support the clinical decision-making process. The ultimate goal of these additions was to evaluate the potential usability and pave the way of automated segmentation methods towards their translation to routine clinical practice.

#### 4.3.1. Assessment of Disease Progression

The inclusion of longitudinal (i.e., follow up) mpMRI scans took place during the BraTS 2014-2016 instances. In clinical practice, assessment of disease progression is to date performed through the Response Evaluation Criteria In Solid Tumours (RECIST) [14-17] and the Response Assessment in Neuro-Oncology (RANO) criteria

[18], whose quantitative component is based on the relative change of tumor size (i.e., percentile changes) measured by the longest two axes of the assessed tumor. In this regard, we postulate that automated algorithms performing brain tumor volumetric segmentation (i.e., in three dimensions) should yield reliable comparable (if not better) estimates of volumetric tumor changes.

#### *4.3.2. Prediction of Overall Survival*

The inclusion of the OS prediction task took place during the BraTS 2017-2018 instances, and has highlighted (or rather confirmed) the difficulties of Deep Learning (DL) approaches to handle small training sets, and the superiority of traditional ML approaches. While this finding clearly calls for larger training sets, it also identifies the need for potential synergies between DL and traditional ML approaches as we transition to larger training sets in the future, which can include more non-uniformly distributed clinical and/or molecular information. In other words, there is a need to develop advanced ML approaches able to handle the large existing heterogeneity of the patient-specific information available in the clinics, e.g., radiogenomics[19-26], RIS reports.

### **4.5. Future Directions for the BraTS Initiative**

The current trend over the years of the previous BraTS instances highlights (or rather confirms) a) the superiority of DL over traditional ML approaches in the segmentation task (and particularly in terms of Dice), and, in contrast, b) the struggle of DL and the superiority of traditional ML approaches, assessing more clinically-relevant problems, such as the prediction of clinical outcome (i.e., overall survival), where smaller training sets are typically available and need to be handled.

Concentrating on the segmentation task, in terms of algorithmic design, the current general consensus seems to point in the direction of tackling the problem in a hierarchical/cascaded way, by first distinguishing between normal and abnormal/tumorous tissue, and then proceeding with the segmentation of the tumor sub-regions. Alternative research directions include the enhancement of the flexibility of DL systems that might lack a given set of input images [27], as a transition measure towards worldwide adoption of the standardization initiatives for GBM imaging [28].

There are many clinical endpoints where the BraTS initiative can have a potential impact and these include, but not limited to: a) training systems for neuroradiology trainees, b) differential diagnosis (e.g., metastases differentiation, disease progression assessment, radio-phenotyping), c) prognosis (e.g., prediction of overall survival, drug-response prediction), d) radiation therapy planning. However, for any of these to be potentially considered wider application of the developed methods needs to take place, which is why we created the BraTS algorithmic repository, and a closer collaboration with the clinical expertise is fundamental to tailor the design of the BraTS challenges towards an effective exploitation and translation of research findings into clinical practice.

## Acknowledgements

Importantly, we would like to express our gratitude to all the data contributing institutions that assisted in putting together the publicly-available multi-institutional mpMRI BraTS dataset, acquired with different clinical protocols and various scanners. Note that without these contributions the BraTS initiative would have never been feasible. These data contributors are: 1) Center for Biomedical Image Computing and Analytics (CBICA), University of Pennsylvania (UPenn), PA, USA, 2) University of Alabama at Birmingham, AL, USA, 3) Heidelberg University, Germany, 4) University Hospital of Bern, Switzerland, 5) University of Debrecen, Hungary, 6) Henry Ford Hospital, MI, USA, 7) University of California, CA, USA, 8) MD Anderson Cancer Center, TX, USA, 9) Emory University, GA, USA, 10) Mayo Clinic, MN, USA, 11) Thomas Jefferson University, PA, USA, 12) Duke University School of Medicine, NC, USA, 13) Saint Joseph Hospital and Medical Center, AZ, USA, 14) Case Western Reserve University, OH, USA, 15) University of North Carolina, NC, USA, 16) Fondazione IRCCS Istituto Neurologico C. Besta, Italy, 17) MD Anderson Cancer Center, TX, USA, 18) Washington University School of Medicine in St. Louis, MO, USA, and 19) Tata Memorial Center, Mumbai, India. Note that data from institutions 6-16 are provided through The Cancer Imaging Archive (TCIA - <http://www.cancerimagingarchive.net/>), supported by the Cancer Imaging Program (CIP) of the National Cancer Institute (NCI) of the National Institutes of Health (NIH).

We would also like to thank the sponsorship offered by the CBICA@UPenn for the plaques provided to the top-ranked participating teams of the challenge each year, as well as Intel AI for sponsoring the monetary prizes of total value of \$5,000, awarded to the three top-ranked participating teams of the BraTS 2018 challenge, who also shared publicly their containerized algorithm in the BraTS algorithmic repository ([https://github.com/BraTS/Instructions/blob/master/Repository\\_Links.md](https://github.com/BraTS/Instructions/blob/master/Repository_Links.md) & <https://hub.docker.com/u/brats/>).

This work was supported in part by the 1) National Institute of Neurological Disorders and Stroke (NINDS) of the NIH R01 grant with award number R01-NS042645, 2) Informatics Technology for Cancer Research (ITCR) program of the NCI/NIH U24 grant with award number U24-CA189523, 3) Swiss Cancer League, under award number KFS-3979-08-2016, 4) Swiss National Science Foundation, under award number 169607.

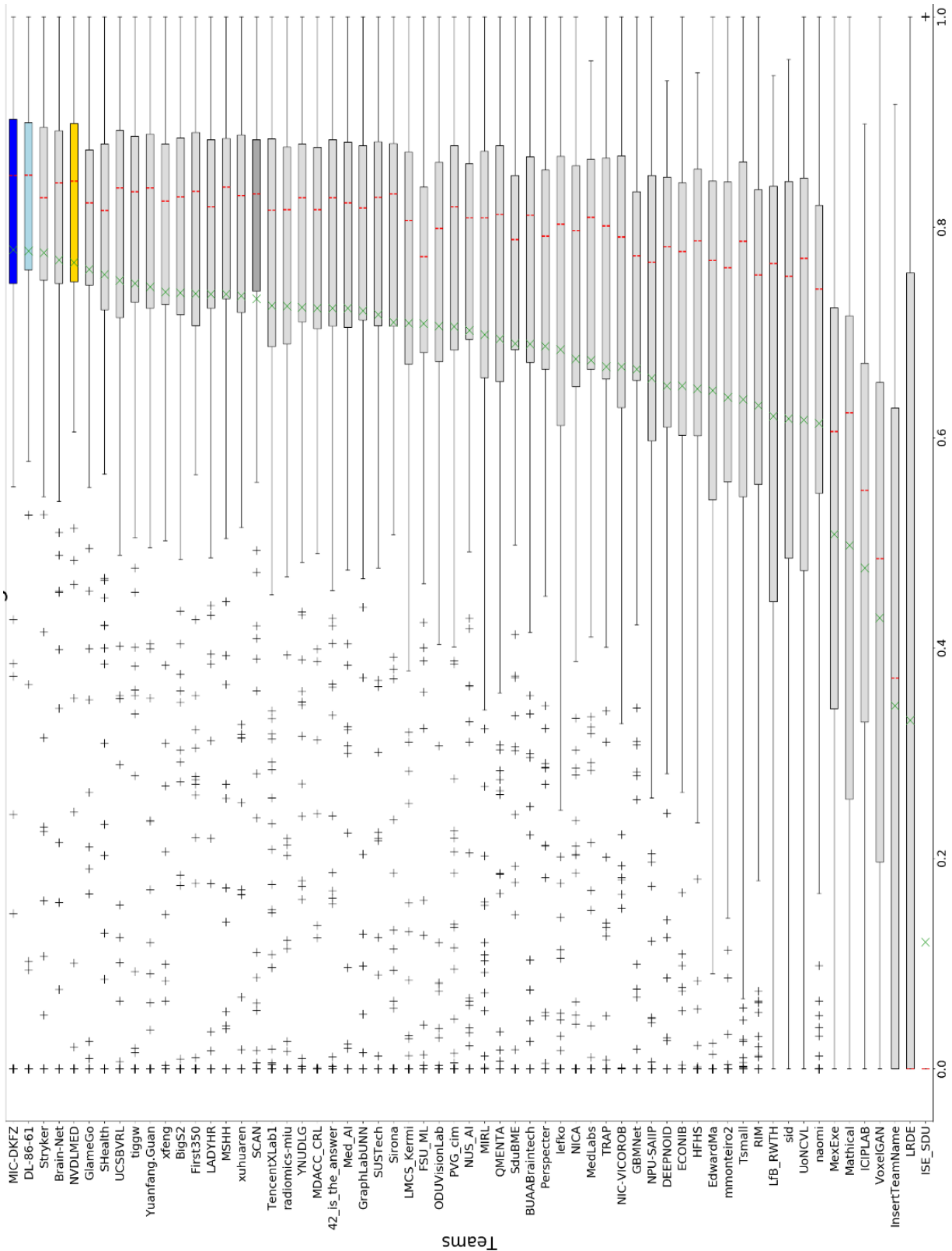
## References

- [1] B. H. Menze, A. Jakab, S. Bauer, J. Kalpathy-Cramer, K. Farahani, J. Kirby, *et al.*, "The Multimodal Brain Tumor Image Segmentation Benchmark (BRATS)," *IEEE Transactions on Medical Imaging*, vol. 34, pp. 1993-2024, 2015.
- [2] S. Bakas, H. Akbari, A. Sotiras, M. Bilello, M. Rozycki, J. S. Kirby, *et al.*, "Advancing The Cancer Genome Atlas glioma MRI collections with expert segmentation labels and radiomic features," *Nature Scientific Data*, vol. 4, p. 170117, 2017
- [3] S. Bakas, H. Akbari, A. Sotiras, M. Bilello, M. Rozycki, J. Kirby, *et al.*, "Segmentation Labels and Radiomic Features for the Pre-operative Scans of the TCGA-LGG collection," T. C. I. Archive, Ed., ed, 2017.
- [4] S. Bakas, H. Akbari, A. Sotiras, M. Bilello, M. Rozycki, J. Kirby, *et al.*, "Segmentation Labels and Radiomic Features for the Pre-operative Scans of the TCGA-GBM collection," T. C. I. Archive, Ed., ed, 2017.
- [5] A. Zwanenburg, S. Leger, M. Vallières, S. Löck, and I. b. s. initiative, "Image biomarker standardisation initiative," *arXiv preprint arXiv:1612.07003*, 2016.
- [6] T. Rohlfing, N. M. Zahr, E. V. Sullivan, and A. Pfefferbaum, "The SRI24 Multi-Channel Atlas of Normal Adult Human Brain Structure," *Human brain mapping*, vol. 31, pp. 798-819, 2010.
- [7] K. Clark, B. Vendt, K. Smith, J. Freymann, J. Kirby, P. Koppel, *et al.*, "The Cancer Imaging Archive (TCIA): Maintaining and Operating a Public Information Repository," *Journal of Digital Imaging*, vol. 26, pp. 1045-1057, 2013.
- [8] L. Scarpace, T. Mikkelsen, S. Cha, S. Rao, S. Tekchandani, D. Gutman, *et al.*, "Radiology Data from The Cancer Genome Atlas Glioblastoma Multiforme [TCGA-GBM] collection," *The Cancer Imaging Archive*, 2016.
- [9] N. Pedano, A. E. Flanders, L. Scarpace, T. Mikkelsen, J. M. Eschbacher, B. Hermes, *et al.*, "Radiology Data from The Cancer Genome Atlas Low Grade Glioma [TCGA-LGG] collection," *The Cancer Imaging Archive*, 2016.
- [10] O. Maier, B. H. Menze, J. von der Gablentz, L. Häni, M. P. Heinrich, M. Liebrand, *et al.*, "ISLES 2015 - A public evaluation benchmark for ischemic stroke lesion segmentation from multispectral MRI," *Medical Image Analysis*, vol. 35, pp. 250-269, 2017/01/01/ 2017.
- [11] S. Winzeck, A. Hakim, R. McKinley, J. A. A. D. S. R. Pinto, V. Alves, C. Silva, *et al.*, "ISLES 2016 and 2017-Benchmarking Ischemic Stroke Lesion Outcome Prediction Based on Multispectral MRI," *Frontiers in neurology*, vol. 9, pp. 679-679, 2018.
- [12] R. Stupp, M. E. Hegi, W. P. Mason, M. J. van den Bent, M. J. B. Taphoorn, R. C. Janzer, *et al.*, "Effects of radiotherapy with concomitant and adjuvant temozolomide versus radiotherapy alone on survival in glioblastoma in a randomised phase III study: 5-year analysis of the EORTC-NCIC trial," *The Lancet Oncology*, vol. 10, pp. 459-466.

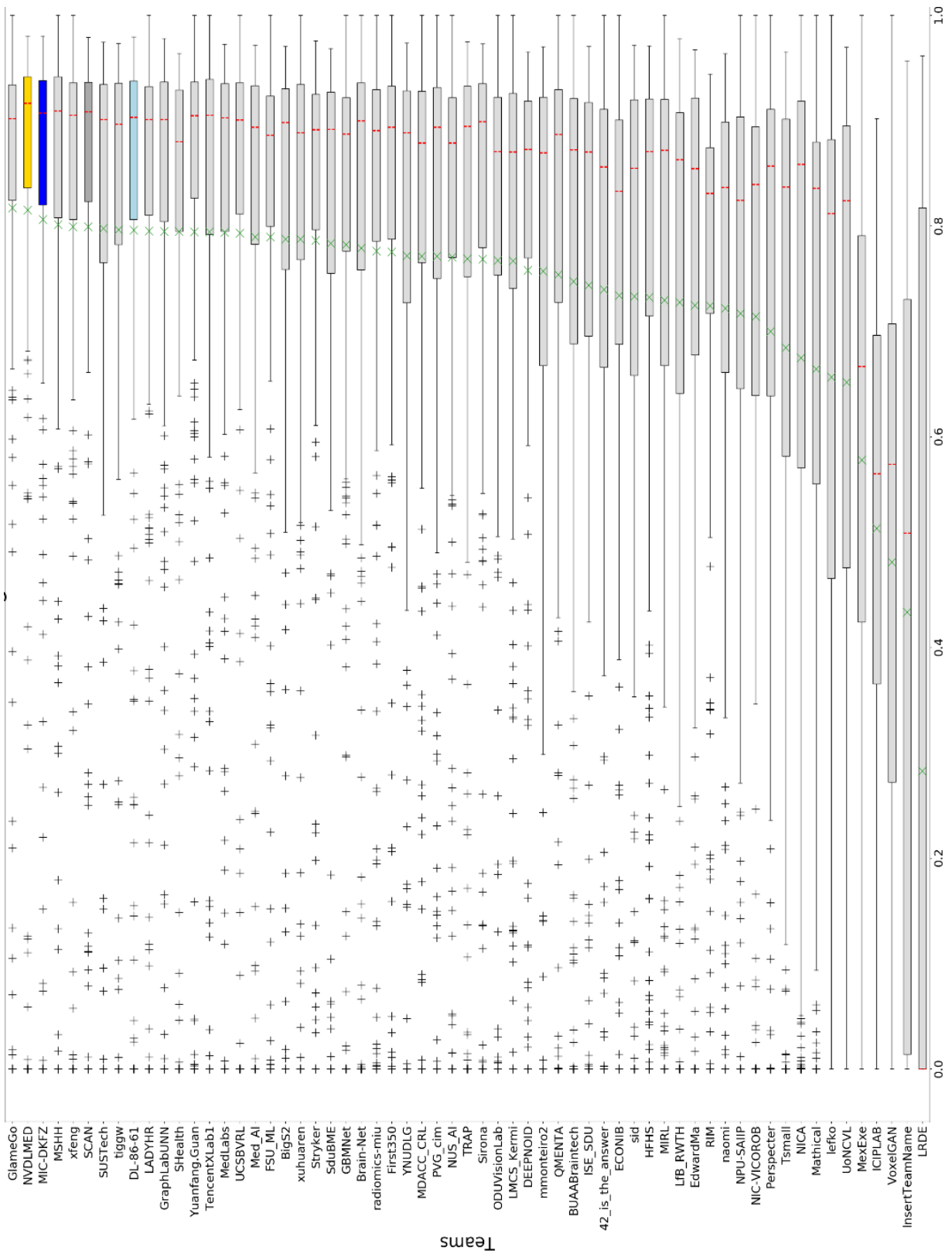
- [13] M. R. Gilbert, M. Wang, K. D. Aldape, R. Stupp, M. E. Hegi, K. A. Jaeckle, *et al.*, "Dose-Dense Temozolomide for Newly Diagnosed Glioblastoma: A Randomized Phase III Clinical Trial," *Journal of Clinical Oncology*, vol. 31, pp. 4085-4091, 2013/11/10 2013.
- [14] Y. Tsuchida and P. Therasse, "Response evaluation criteria in solid tumors (RECIST): New guidelines," *Medical and Pediatric Oncology*, vol. 37, pp. 1-3, 2001.
- [15] E. A. Eisenhauer, P. Therasse, J. Bogaerts, L. H. Schwartz, D. Sargent, R. Ford, *et al.*, "New response evaluation criteria in solid tumours: revised RECIST guideline (version 1.1)," *European journal of cancer*, vol. 45, pp. 228-247, 2009.
- [16] E. L. v. P. van Meerten, H. Gelderblom, and J. L. Bloem, "RECIST revised: implications for the radiologist. A review article on the modified RECIST guideline," *European radiology*, vol. 20, pp. 1456-1467, 2010.
- [17] B. M. Ellingson, P. Y. Wen, and T. F. Cloughesy, "Modified Criteria for Radiographic Response Assessment in Glioblastoma Clinical Trials," *Neurotherapeutics : the journal of the American Society for Experimental NeuroTherapeutics*, vol. 14, pp. 307-320, 2017.
- [18] P. Y. Wen, D. R. Macdonald, D. A. Reardon, T. F. Cloughesy, A. G. Sorensen, E. Galanis, *et al.*, "Updated Response Assessment Criteria for High-Grade Gliomas: Response Assessment in Neuro-Oncology Working Group," *Journal of Clinical Oncology*, vol. 28, pp. 1963-1972, 2010.
- [19] K. Chang, H. X. Bai, H. Zhou, C. Su, W. L. Bi, E. Agbodza, *et al.*, "Residual Convolutional Neural Network for the Determination of  $IDH$  Status in Low- and High-Grade Gliomas from MR Imaging," *Clinical Cancer Research*, vol. 24, pp. 1073-1081, 2018.
- [20] H. Itakura, A. S. Achrol, L. A. Mitchell, J. J. Loya, T. Liu, E. M. Westbroek, *et al.*, "Magnetic resonance image features identify glioblastoma phenotypic subtypes with distinct molecular pathway activities," *Science Translational Medicine*, vol. 7, pp. 303ra138-303ra138, 2015.
- [21] S. Bakas, H. Akbari, J. Pisapia, M. Martinez-Lage, M. Rozycki, S. Rathore, *et al.*, "In vivo detection of EGFRvIII in glioblastoma via perfusion magnetic resonance imaging signature consistent with deep peritumoral infiltration: the  $\phi$ -index," *Clinical Cancer Research*, vol. 23, pp. 4724-4734, 2017.
- [22] H. Akbari, S. Bakas, J. M. Pisapia, M. P. Nasrallah, M. Rozycki, M. Martinez-Lage, *et al.*, "In vivo evaluation of EGFRvIII mutation in primary glioblastoma patients via complex multiparametric MRI signature," *Neuro-Oncology*, vol. 20, pp. 1068-1079, 2018.
- [23] Z. A. Binder, A. H. Thorne, S. Bakas, E. P. Wileyto, M. Bilello, H. Akbari, *et al.*, "Epidermal Growth Factor Receptor Extracellular Domain Mutations in Glioblastoma Present Opportunities for Clinical Imaging and Therapeutic Development," *Cancer Cell*, vol. 34, pp. 163-177.e7, 2018/07/09/ 2018.
- [24] B. M. Ellingson, "Radiogenomics and imaging phenotypes in glioblastoma: novel observations and correlation with molecular characteristics.," *Curr Neurol Neurosci Rep*, vol. 15, p. 506, 2015.
- [25] A. M. Rutman and M. D. Kuo, "Radiogenomics: Creating a link between molecular diagnostics and diagnostic imaging," *European Journal of Radiology*, vol. 70, pp. 232-241, 5// 2009.

- [26] M. Nicolasjilwan, Y. Hu, C. Yan, D. Meerzaman, C. A. Holder, D. Gutman, *et al.*, "Addition of MR imaging features and genetic biomarkers strengthens glioblastoma survival prediction in TCGA patients," *Journal of Neuroradiology*, vol. 42, pp. 212-221, 7// 2015.
- [27] M. Havaei, N. Guizard, N. Chapados, and Y. Bengio, "HeMIS: Hetero-Modal Image Segmentation," Cham, 2016, pp. 469-477.
- [28] B. M. Ellingson, C. the Jumpstarting Brain Tumor Drug Development Coalition Imaging Standardization Steering, M. Bendszus, C. the Jumpstarting Brain Tumor Drug Development Coalition Imaging Standardization Steering, J. Boxerman, C. the Jumpstarting Brain Tumor Drug Development Coalition Imaging Standardization Steering, *et al.*, "Consensus recommendations for a standardized Brain Tumor Imaging Protocol in clinical trials," *Neuro-Oncology*, vol. 17, pp. 1188-1198, 2015.

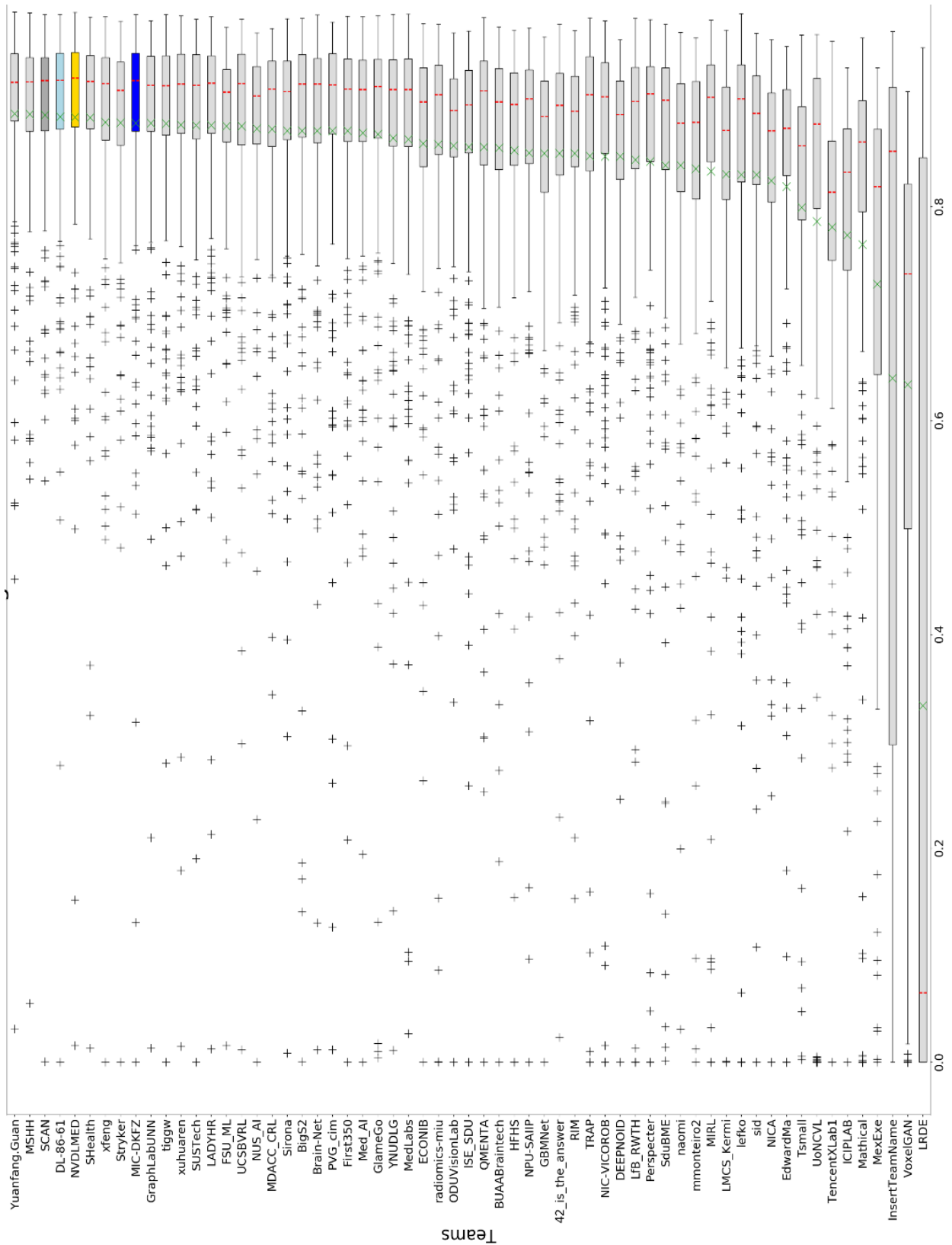
# Supplementary Material



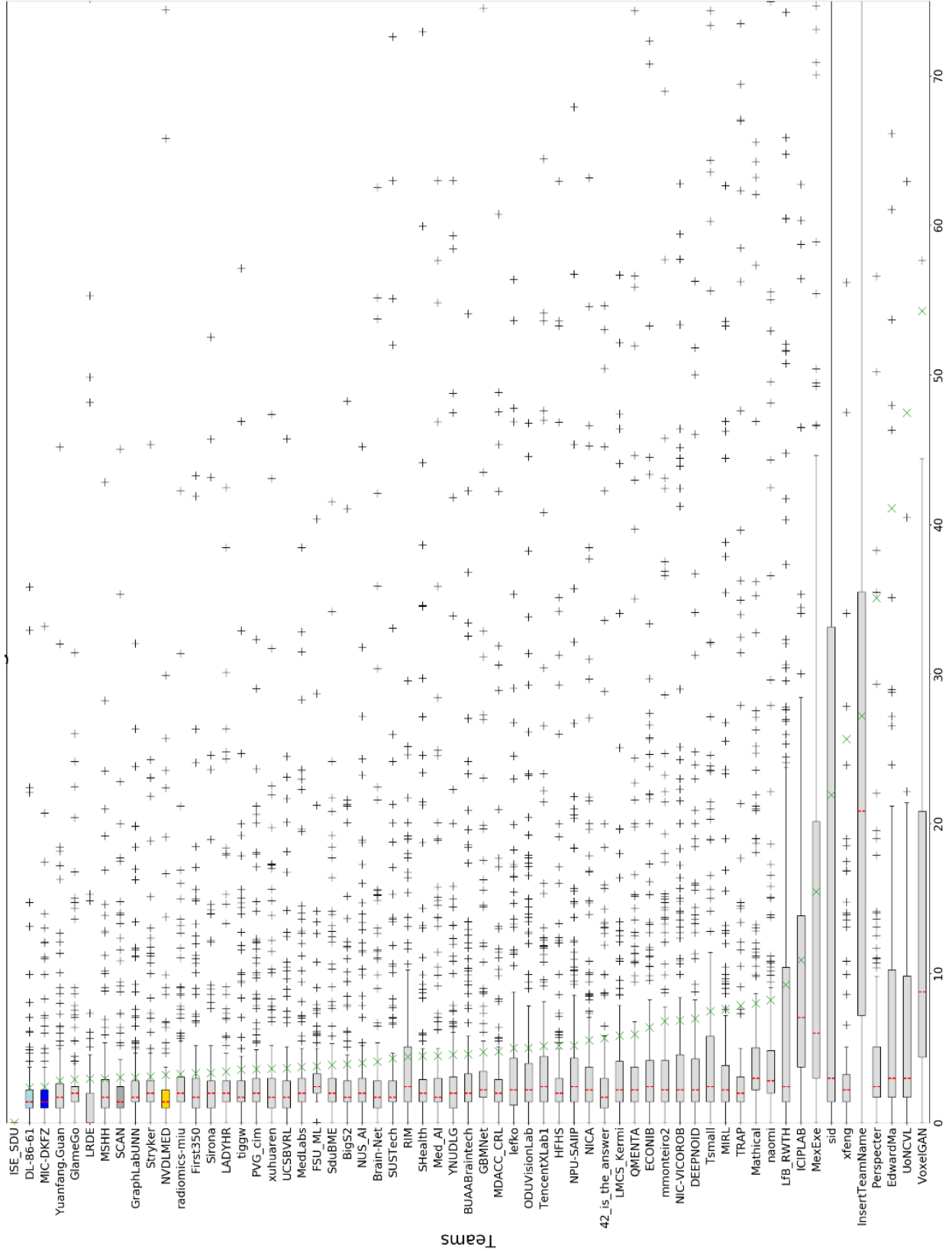
Suppl. Figure 1. BraTS 2018 summarizing results (Dice) for the segmentation of the active tumor compartment.



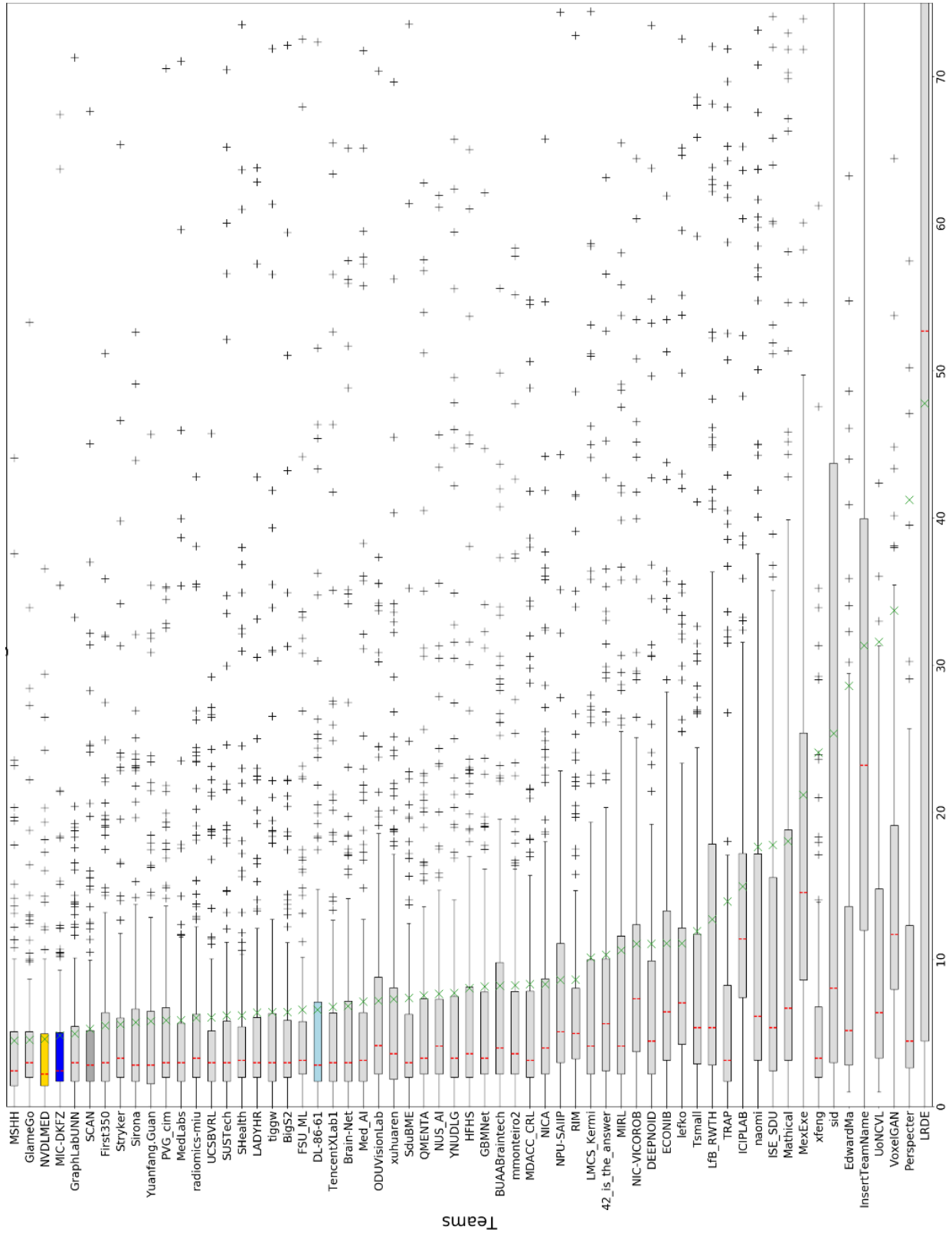
Suppl. Figure 2. BraTS 2018 summarizing results (Dice) for the segmentation of the tumor core compartment.



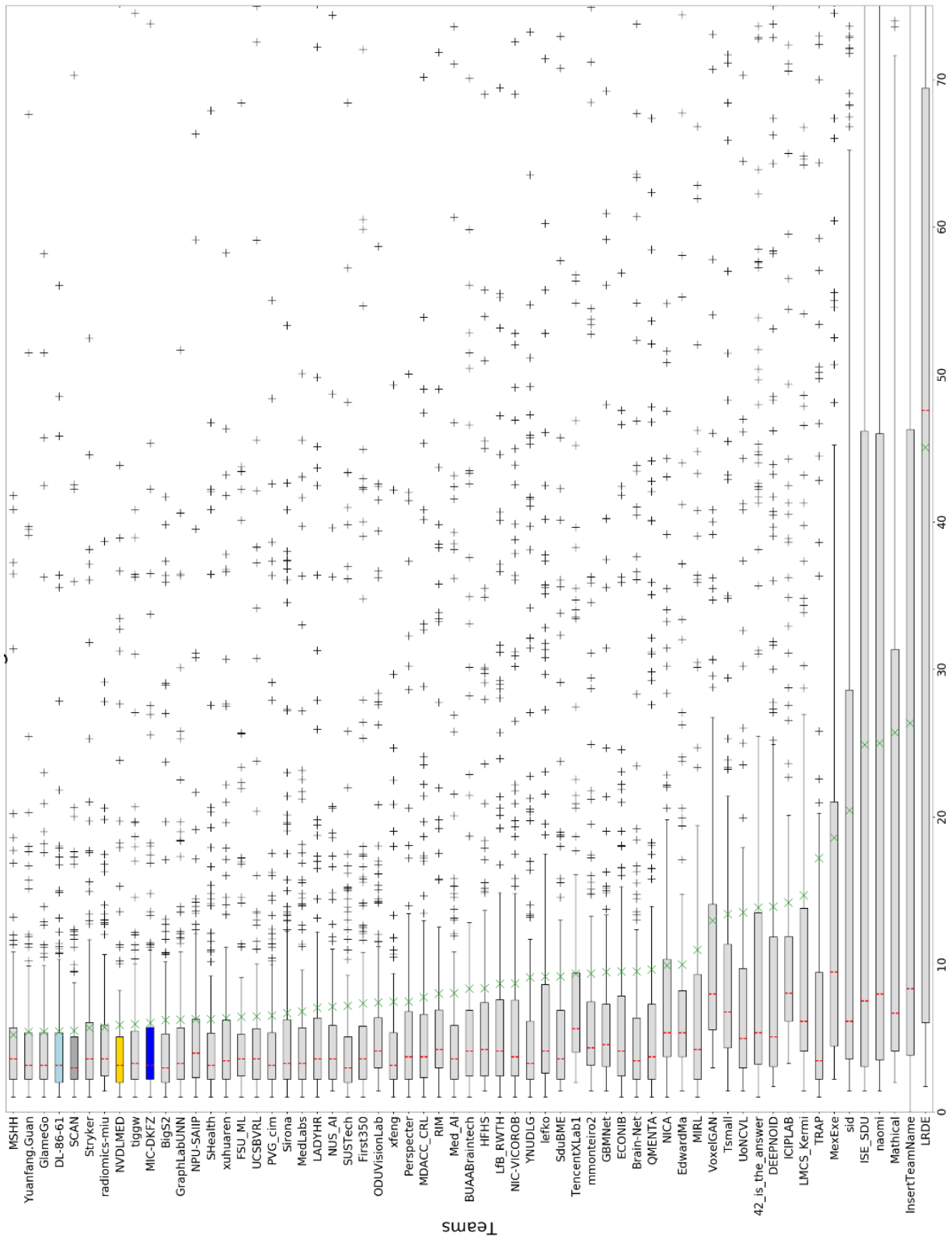
Suppl. Figure 3. BrATS 2018 summarizing results (Dice) for the segmentation of the whole tumor compartment.



Suppl. Figure 4. BraTS 2018 summarizing results (Hausdorff) for the segmentation of the active tumor compartment.



Suppl. Figure 5. BraTS 2018 summarizing results (Hausdorff) for the segmentation of the tumor core compartment.



Suppl. Figure 6. BraTS 2018 summarizing results (Hausdorff) for the segmentation of the whole tumor compartment.